Chelyabinsk Physical and Mathematical Journal. 2025. Vol. 10, iss. 4. P. 801–812.

DOI: 10.47475/2500-0101-2025-10-4-801-812

MOLECULAR DYNAMICS SIMULATIONS OF TAYLOR IMPACT TESTS WITH CLASSICAL AND PROFILED COPPER CYLINDERS

A.E. Mayer[a], E.S. Rodionov[b], V.V. Pogorelko[c], P.N. Mayer[d]

Chelyabinsk State University, Chelyabinsk, Russia
[a]mayer@csu.ru, [b]rodionoves.pgd@gmail.com, [c]vik_ko83@mail.ru, [d]polina.nik@mail.ru

Taylor tests suggesting a high-velocity impact of specimens on a rigid anvil are widely used to study dynamic response of various metallic materials. In order to extend our previous experimental investigations and to reveal the features of Taylor tests at nanoscale, here we perform molecular dynamics simulations for single crystalline and polycrystalline copper considering both classical cylindrical samples and profiled ones with the reduced head part. The sample shapes are similar to that used in experiments, but the total length is 80 or 200 nm in contrast to 40-mm-length samples in the experiments. In spite of five orders of magnitude difference in length, the MD-calculated curves of the normalized length after impact versus the impact velocity are similar to that experimentally measured for millimeter samples, but, as expected, reveal much higher strength of nanoscale samples. Both single crystalline and polycrystalline samples are subjected to loss of the initial cylindrical symmetry in the course of impact. In the case of single crystal, this is due to activation of certain slip systems. In the case of polycrystals, this is connected with the anisotropy of individual grains and is clearly evident when the profiled part of the sample contains only a few grains in the thickness direction. This loss of the symmetry correlates with the distortion of the shape of the profiled samples in our experiments with annealed coarse-grained copper, in which the largest grains reach millimeter sizes. Thus, the symmetry distortion observed in the experiment has a fundamental reason of the deformation localization.

Keywords: *Taylor impact test, nanoscale sample, molecular dynamics, dynamic plastic deformation, copper, single crystal, polycrystal, loss of symmetry, plastic flow localization.*

Introduction

Taylor tests suggesting a high-velocity impact of specimens on a rigid anvil are widely used to study dynamic response of various metallic materials, including ordinary metals [1–3] and alloys [4–6], as well as additively manufactured alloys [7–9] and high-entropy alloys [10–12]. This is a standard experimental technique to extract dynamic yield strength at strain rates of the order of 10^4–$10^5\,\mathrm{s}^{-1}$ [13] and to optimize material model parameters [14; 15] including the application of machine learning methods [16–18]. Typical sizes of the impacted samples in these studies are several millimeters in diameter and tens of millimeters in length characterizing the macroscopic plasticity and fracture response. Classical uniform cylinders are commonly used as the investigated samples in the Taylor impact tests, while profiling of the head part of the impacted samples allows

This research was funded by the Russian Science Foundation, Project No. 20-11-20153-P, https://rscf.ru/en/project/23-11-45024/.

one to concentrate the kinetic energy and to increase the strain rates and strain values [5; 13; 18].

Recently, microscale dynamic testing gain substantial attention [19], including the laser-induced particle impact test [20–22], which applies spherical particles with diameters of about tens of micrometers accelerated by nanosecond laser pulses through ablation and expansion of a nanometers-thick gold film and a micrometers-thick polyurethane film deposited on a glass substrate. The particle velocity varies from tens of meters per second up to several kilometers per second providing severe plastic deformation of a softer material at a strain rate up to $10^8\,\mathrm{s}^{-1}$ [23]. This technique can be used to study both the dynamic property of particle material if the target material is harder and the dynamic property of target material in the opposite case [20]. When considering the microscale samples and even more so the nanoscale samples, an important issue is the transferability of macroscopic properties. In this sense, study on the impact behavior of nanoscale samples in Taylor anvil tests with the help of molecular dynamics (MD) simulations is a relevant topic, although it has not been addressed in the existing literature to the best of our knowledge.

Taylor impact tests with single crystal tantalum samples [1] reveal strong anisotropy with respect to the impact direction and loss of the initial symmetry due to the strain localization. These features are the challenges for macroscopic plasticity theories and attracts substantial modeling efforts [24; 25] in the frames of crystal plasticity combined with the finite element calculations. Polycrystalline materials are assumed to have an averaged properties and not so prone to anisotropic behavior, but it can be the case for coarse grained annealed materials with the grain size comparable with the sample dimensions. For instance, our previous experiments with cold-rolled [2; 13; 18] and annealed copper samples reveal much stronger bending of the head part of profiled samples in the case of annealed copper with the average grain size of about 300 μm (only 5–10 grains per the diameter of the head part) compared with the cold-rolled copper with the average grain size of 18 μm (about hundred of grains across the head part). Our present MD simulations show that this behavior has a fundamental origin from the anisotropy of individual grains, which, in the case of small number of grains across the impactor head part leads to the strain localization and the loss of symmetry similar to the case of single crystals.

Considering all above motivation and supplementing our previous experimental program for copper [2; 13; 18], here we perform MD simulations of the Taylor impact tests for monocrystalline and polycrystalline copper samples, which are geometrically similar to the experimental ones, but having a length of 80 or 200 nm in contrast to 40-mm-long samples in the experiments. Both classical uniform cylinders and that with the profiled head part are considered. The impact velocity range is close to that in our experiments.

1. MD problem statement

Classical MD simulations are performed with the widely used Large-scale Atomic/Molecular Massively Parallel Simulator (LAMMPS) [26; 27], which now is the standard software in the most of MD simulations. Well-approved classical interatomic potential [28] of the embedded atom model (EAM) type [29] is used for Cu–Cu interactions. To analyze the calculated atomic configurations, the OVITO software [30] is applied, which implements, in particular, the dislocation extraction algorithm (DXA) [31] and the polyhedral template matching algorithm [32].

The examined MD systems are shown in Fig. 1 and include small monocrystalline

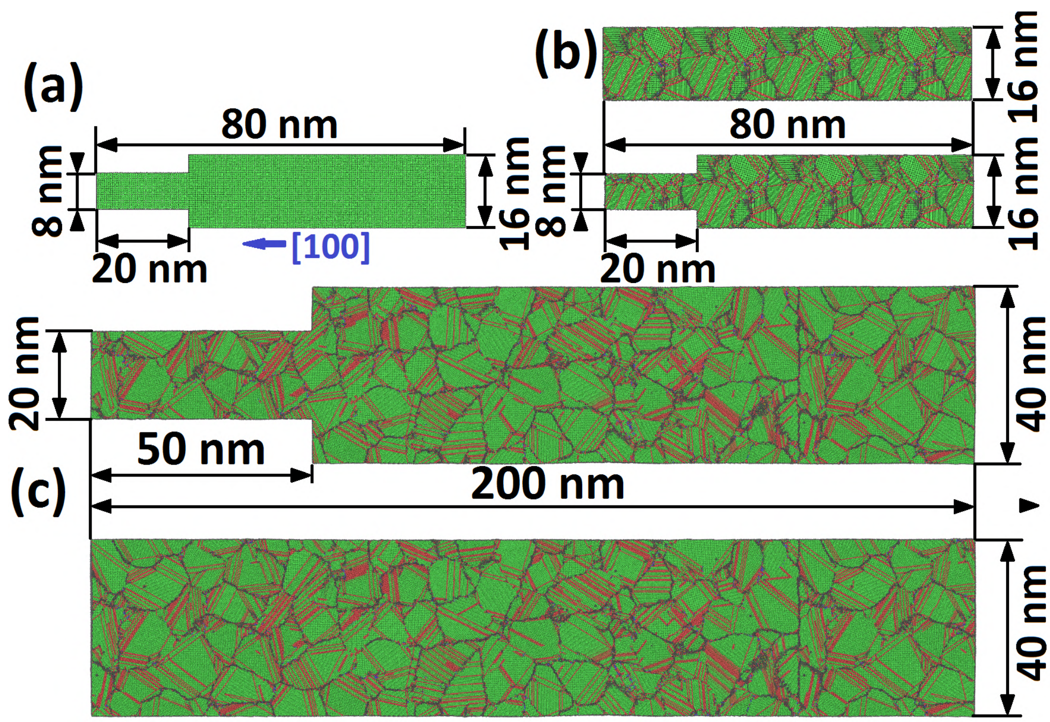

Fig. 1. Studied MD systems: (a) single crystal with 1.1 million atoms, (b) small polycrystal with 1.09 million atoms (profiled cylinder) or 1.34 million atoms (uniform cylinder) and (c) large polycrystal with 17.1 million atoms (profiled cylinder) or 21 million atoms (uniform cylinder). The color coding is described in Figs. 2–5; central sections are shown

and polycrystalline copper samples with the length of 80 nm and the number of atoms of about 1.1–1.3 millions (Fig. 1, *a,b*), as well as large polycrystalline copper samples with the length of 200 nm and the number of atoms in the range of 17–21 millions (Fig. 1, *c*). In the case of polycrystalline copper, we consider both classical uniform cylinders and profiled cylinders with the reduced head part. In the case of copper single crystals, only profiled samples are analyzed. The MD-considered samples are geometrically similar to that were experimentally examined [2; 13; 18], but reduced in $5 \cdot 10^5$ or $2 \cdot 10^5$ times for small and large MD systems, respectively.

The lattice direction [100] of single crystals is directed along the cylinder axis as shown in Fig. 1, *a*. To prepare the polycrystalline models, preliminary MD simulations of melting and crystallization were performed. In the case of large polycrystalline models, a copper single crystal with the dimensions of 200 nm × 45 nm × 45 nm was molten at high temperature and, thereafter, was cooled and crystallized with introducing of randomly oriented and randomly located crystallization centers maintained at low temperature. As a result, a polycrystalline bar was obtained containing 830 grains with an average grain diameter of about 8 nm, from which the classical and profiled cylinders were cut out. In the case of small polycrystalline samples, a smaller single crystal with dimensions of 20 nm × 20 nm × 20 nm was molten and crystallized on 9 crystallization centers providing a close grain size. The small crystallized cube was replicated four time to reach the total length of 80 nm and, thereafter, the required sample shape was cut out. This preparation procedure leads to periodically repeating grain structure of small polycrystalline samples, but does not influence the average mechanical response as shown below. As shown in Fig. 1, the monocrystalline samples have a perfect initial crystal structure of face-centered cubic (FCC) lattice, while the polycrystalline samples reveal a large number of grain boundaries and intra-grain stacking faults indicating the traces of plastic deformation at crystallization and thermal shrinkage.

After relaxation and thermalization at 300 K, an initial velocity directed along the cylinder axis toward the rigid anvil is set to the sample by adding this ordered velocity to the thermal velocity of each atom. Periodic boundary conditions in all directions act during the relaxation stage; thereafter, they are replaced by free (shrink-wrapped) boundaries from all sides except the anvil side. The rigid anvil is modeled by fixed boundary condition, leading to the momentum reflection of the atoms in contact with this boundary (the imaginary anvil surface). The collision of sample with anvil is simulated in microcanonical (NVE) ensemble with the conservation of total energy. The investigated range of impact velocities with the maximal velocity of 180 m/s is somewhat wider than that investigated in the experiments [2; 13; 18].

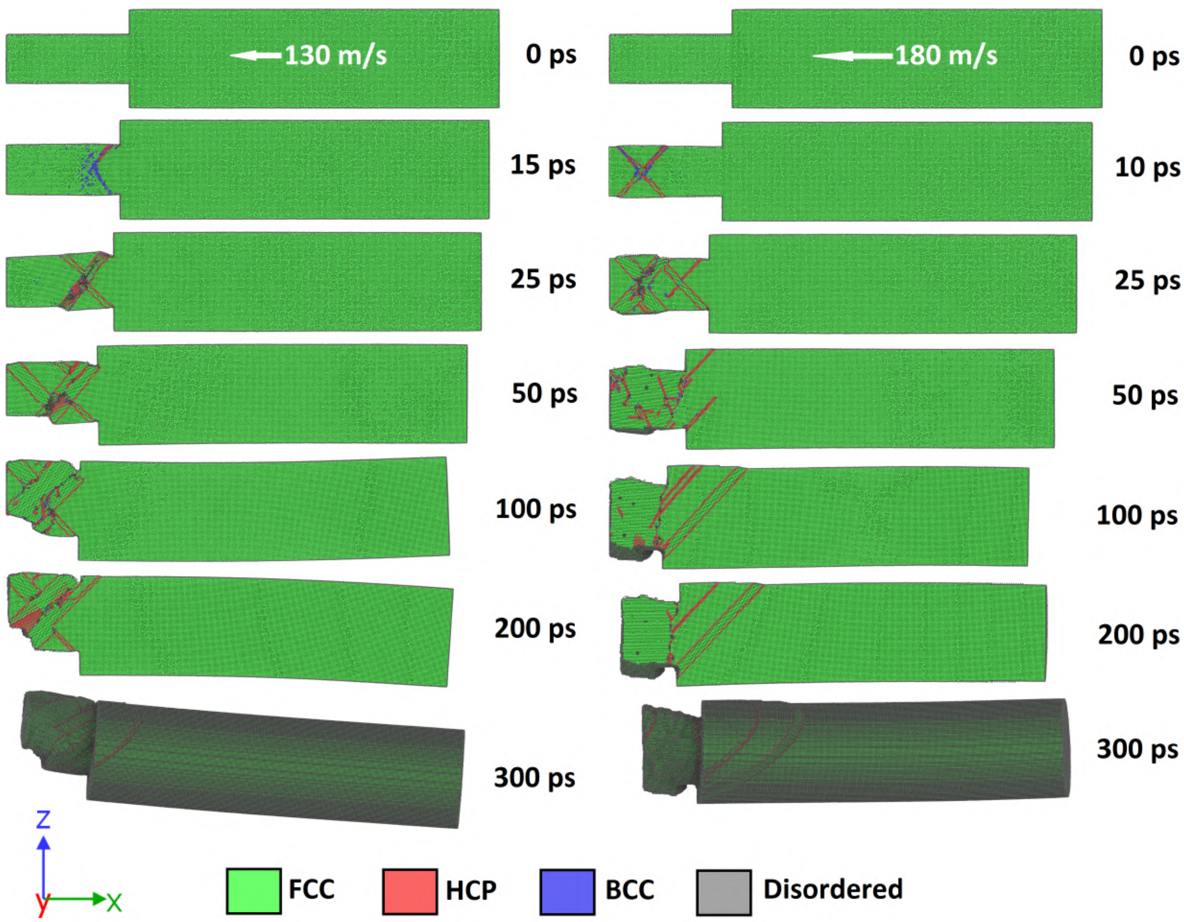

Fig. 2. Impact of profiled 80-nm-long monocrystalline samples at the impact velocity of 130 m/s (left column) and 180 m/s (right column). All plots besides the bottom ones present central section of the sample; atoms are colored in accordance with the local ordering as described by the legend

2. Dynamic deformation of nanoscale samples

Fig. 2 shows dynamic deformation of single crystal copper at two impact velocities. The plastic deformation starts with nucleation and propagation of Shockley partial dislocations leaving the staking faults indicated in Fig. 2 as the stripes of hexagonal closed packed (HCP) atoms. In contrast to the case of homogeneous nucleation of dislocations in the bulk of material [33], the dislocations are emitted from the lateral surface of the reduced cylindrical head part. Similar to that was reported previously [34; 35], a fraction of bulk-centered cubic (BCC)-ordered atoms appears before the dislocation emission indicating an unstable state of the crystal lattice under imposed elastic deformation. The emitted dislocations form slip bands in (111) closed packed planes crossing the head part and leading to the strain localization, which, in turn, leads to the loss of cylindrical symmetry of the samples and to an oblique rebound at the late stage of collision. The plastic deformation is mainly concentrated in the reduced head part, but it touches the main part of the cylinder as well providing steps on the lateral surface, ending the slip bands.

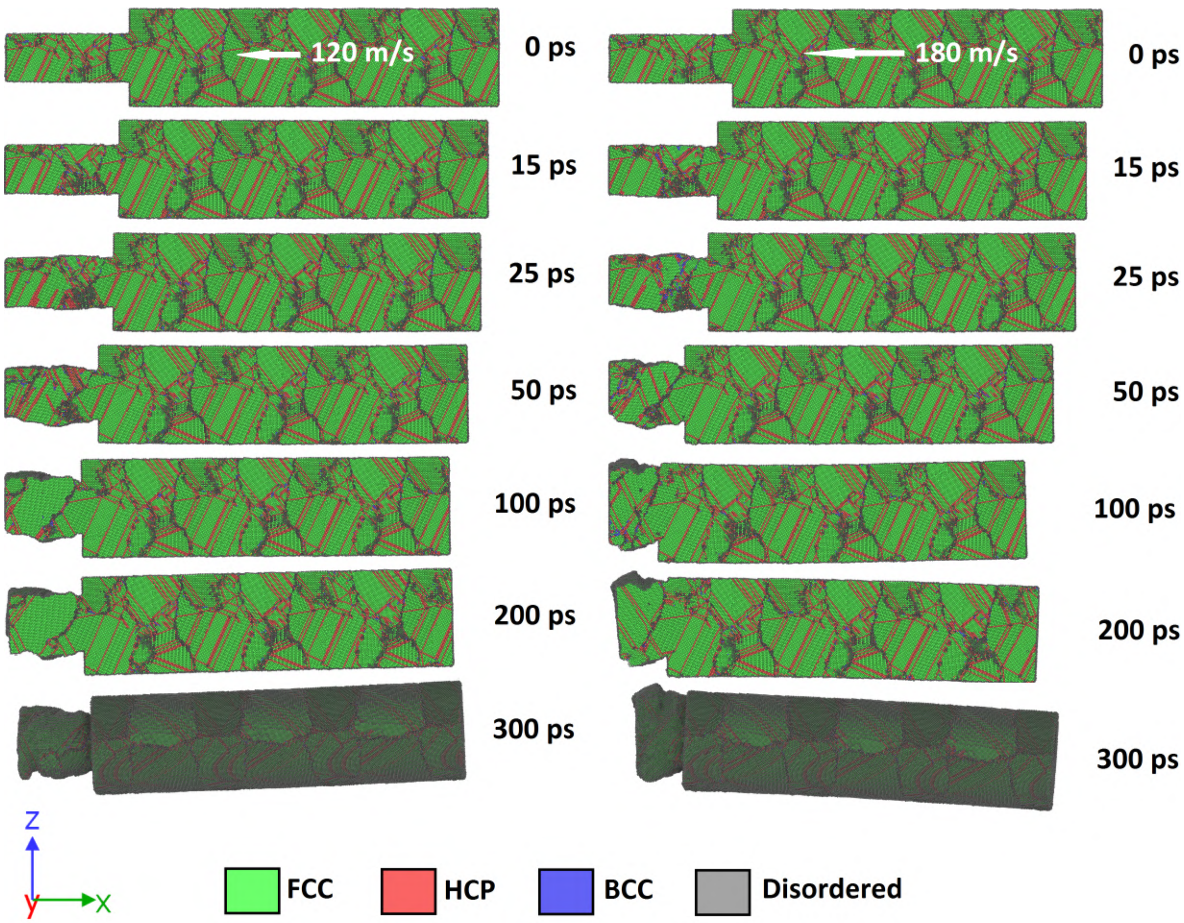

Fig. 3. Impact of 80-nm-long profiled polycrystalline samples at the impact velocity of 120 m/s (left column) and 180 m/s (right column). All plots besides the bottom ones present central section of the sample; atoms are colored in accordance with the local ordering as described by the legend

The polycrystalline samples shown in Fig. 3 have initial abundant defect substructure. As a result, there is no need to accumulate high elastic stresses required to trigger the dislocation nucleation/emission, and the plastic deformation starts earlier compared to the case of single crystals. Nevertheless, further evolution and the final shapes are very similar, compare Fig. 3 and Fig. 2. Polycrystalline samples are also prone to the strain localization and the oblique rebounding, just like single crystals. For the profiled small polycrystalline models, the diameter of the reduced head part is about the grain size. Therefore, the anisotropy of the elastic properties and the plastic slip of particular grains in the head part are significant and not properly averaged through a number of grains resulting in the loss of the initial cylindrical symmetry.

Fig. 4 shows the case of classical uniform cylinders traditionally applied in the Taylor impact tests. This is a small polycrystalline copper model. One can see that the final plastic deformation is much weak compared with the case of profiled samples in Fig. 3 at the same impact velocities. This difference motivated us to develop the profiled cylinders [18] in order to concentrate the kinetic energy in a small head part and to increase the reached deformation degree. In spite of a weaker deformation and a higher number of grains per cross-section, the uniform cylinders are also prone to the loss of axial symmetry and to an oblique rebounding, although in a lesser degree than in the case of profiled ones.

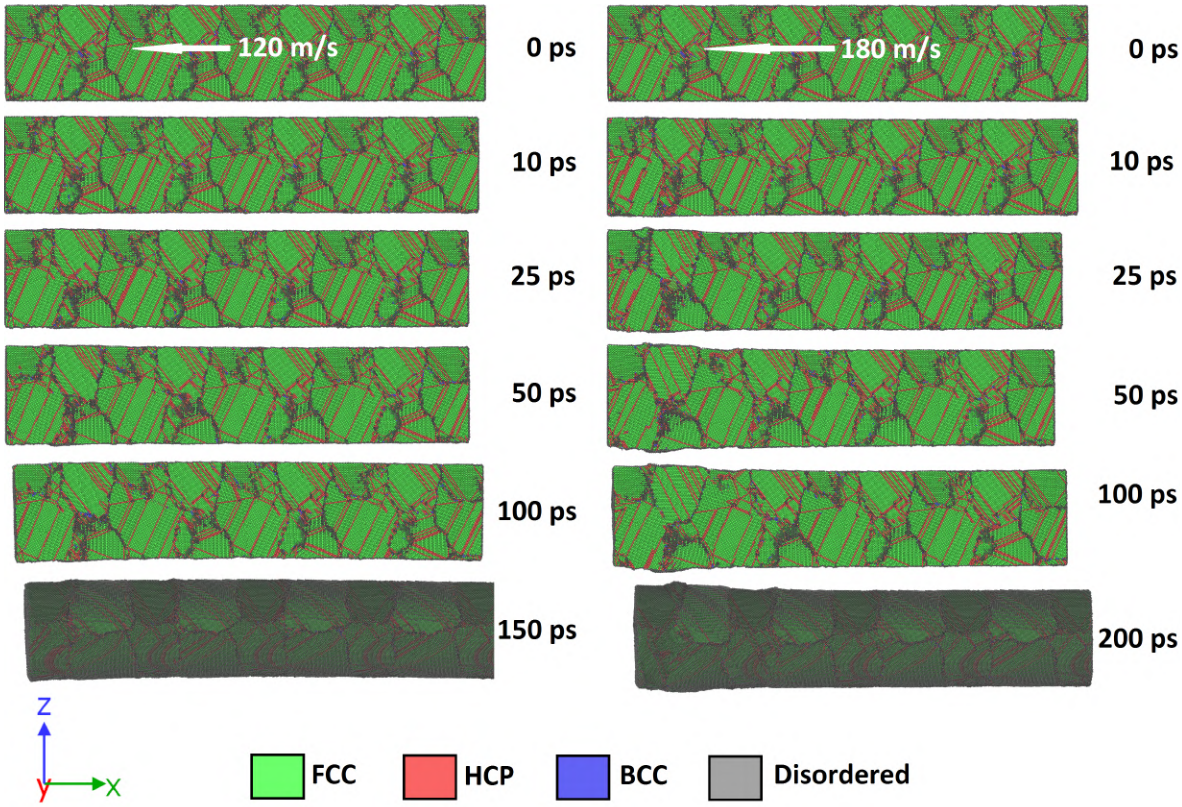

Fig. 4. Impact of the classical uniform cylinders 80 nm in length made of polycrystalline copper at the impact velocity of 120 m/s (left column) and 180 m/s (right column). All plots besides the bottom ones present central section of the sample; atoms are colored in accordance with the local ordering

As far as the number of grains is very limited at the impact edge of the small polycrystalline model, which can distort the deformation process, a larger polycrystalline model shown in Fig. 1, *c* was constructed and examined; the results are shown in Fig. 5. The increase in the number of grains really increases the uniformity, but does not completely eliminate the bending of the heat part and the oblique rebounding. Even for this large polycrystalline model, there are still only about 3–5 grains per the diameter of the impact edge, retaining the large influence of the plastic deformation anisotropy of particular grains.

We can conclude that there is a fundamental reason for the loss of the initial symmetry and for the oblique rebounding even for the geometrically perfect initial shape and for the normal impact. Therefore, the bending of the samples in the experiment is not always because of inaccurate experimental scheme, but can come from the features of the material microstructure. This conclusion is in line with the experimental results for macroscopic samples made of tantalum single crystals, for which strong anisotropy, strain localization and loss of symmetry were reported [1] and confirmed by the crystal plasticity calculations [24; 25]. This is also in line with our recent experimental results for cold-rolled [2; 13; 18] and annealed copper samples, which revealed much stronger bending of the head part of profiled samples in the case of annealed copper compared with the as-received cold-rolled ones. This can be explained by a large grain size of about 300 μm in the annealed copper, which results in 5–10 grains per the diameter of the head part, compared with the cold-rolled copper with the average grain size of 18 μm providing about hundred of grains across the head part and leading to an efficient averaging of material properties. On the other hand, the strain localization obviously takes place even for fine-grained materials, in particular at the initiation of fracture [5].

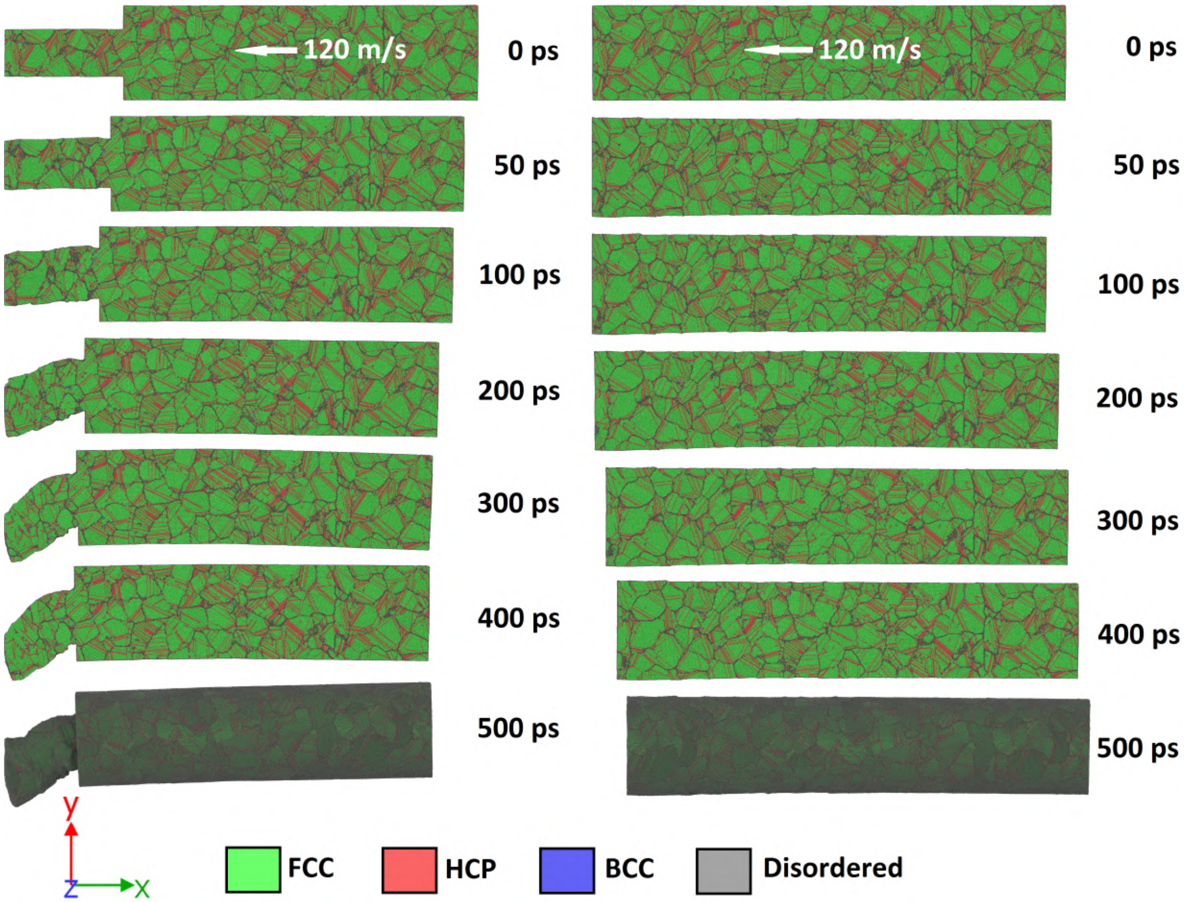

Fig. 5. MD results for large polycrystalline model: Impact of profiled (left column) and classical uniform (right column) cylinders 200 nm in length at the impact velocity of 120 m/s. All plots besides the bottom ones present central section of the sample; atoms are colored in accordance with the local ordering as described by the legend

3. Comparison with experiments for macroscopic samples

Fig. 6 summarizes the change in length of all MD-simulated samples versus the impact velocity. In order to compare the different-scale impactors, the ratio of the final length to the initial one (the normalized length) is used as the measure of the final plastic deformation. Fig. 6, *b* shows that all three studied types of MD systems, single crystals, small polycrystals and large polycrystals, reveal the same deformation behavior, and the corresponding data points lay around the same dependence fitted to the small polycrystals taking into account a certain statistical straggling. It is remarkable that both the perfect single crystals and the defect-reach polycrystals experience very similar final deformation, in spite of the fact that the dislocation emission triggers the plastic deformation in the former case, while the activation of the existing defects is the prevalent mechanism in the later case. This feature indicates that the system loses the memory of the plasticity incipience. Fig. 6, *a* for classical uniform cylinders shows very close final deformation of both small and large polycrystals.

MD results in Fig. 6 are compared with our recent experimental data [2; 13; 18] for the cold-rolled copper samples with the length of 40 mm. In spite of five orders of magnitude difference in length, the MD-calculated curves are similar to that experimentally measured for the millimeter samples, but, as expected, reveal much higher strength of the nanoscale samples. The higher strength of nanoscale systems can be explained by two factors. The first one is much higher strain rates at deformation. Figs. 2 and 3 show that the main stage of the deformation of the head part lasts for about 100 ps reaching the deformation degree of about 1, which gives an estimate of $10^{10}\,s^{-1}$ for the average strain rate, while it is only about 10^4–$10^5\,s^{-1}$ in the case of experiment [2; 13; 18]. Such increase in the strain rate substantially enhances the yield strength. Another factor is the small grain/sample size, which restricts the free path of dislocations before the disappearance or pinning at grain boundaries or lateral surfaces, which is the leading mechanism of the strengthening of nanoscale systems.

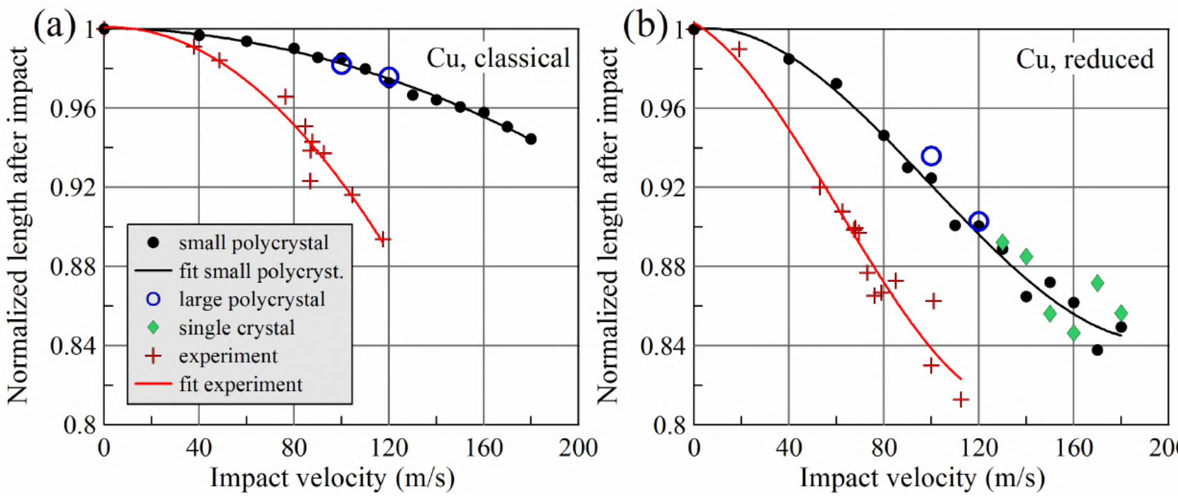

Fig. 6. Comparison of MD results for nanoscale samples with the experimental data [2; 18] for macroscopic samples: Normalized length of the deformed samples in the case of (a) classical cylinders and (b) profiled cylinders with the reduced head part

Remarkably, the scatter of experimental data points around the fitted curves in Fig. 6 is comparable with that is observed for the MD-calculated data points. It means that the experimentally measured scatter can be partially explained by some fundamental reasons, including variation of the material microstructure and properties.

Conclusions

For extension of our previous experimental investigations and revealing the features of Taylor impact tests at nanoscale, here we perform MD simulations for single crystalline and polycrystalline copper considering both classical cylindrical samples and profiled ones with the reduced head part. The sample shapes are similar to that used in experiments, but the total length is 80 or 200 nm in contrast to 40-mm-length samples in the experiments. In spite of five orders of magnitude difference in length, the MD-calculated curves of the normalized length after impact versus the impact velocity are similar to that experimentally measured for macroscopic samples, but reveal much higher strength of nanoscale samples. The enhanced strength is due to both much higher strain rate and smaller free paths of dislocations in the nanoscale impactors. Both single crystalline and polycrystalline samples are subjected to loss of the initial cylindrical symmetry in the course of impact. In the case of single crystal, this is due to activation of certain slip systems. In the case of polycrystals, this is connected with the anisotropy of individual grains and is clearly evident when the profiled part of the sample contains only a few grains in the thickness direction. This loss of the symmetry correlates with the distortion of the shape of the profiled samples in our experiments with annealed coarse-grained copper, in which the largest grains reach millimeter sizes. Thus, the symmetry distortion observed in the experiment has a fundamental reason of the plastic flow localization. Besides, our idealized consideration in the MD reveals a scatter of deformation results along some general trend, suggesting fundamental reasons of similar scatter observed in the experiments. An obvious fundamental reason is variation of the material microstructure and properties.

References

1. **Lim H., Carroll J.D., Battaile C.C., Chen S.R., Moore A.P., Lane J.M.D.** Anisotropy and strain localization in dynamic impact experiments of tantalum single crystals. *Scientific Reports*, 2018, vol. 8, p. 5540.
2. **Rodionov E.S., Lupanov V.G., Grachyova N.A., Mayer P.N., Mayer A.E.** Taylor impact tests with copper cylinders: experiments, microstructural analysis and 3D SPH modeling with dislocation plasticity and MD-informed artificial neural network as equation of state. *Metals*, 2022, vol. 12, no. 2, p. 264.
3. **Zelepugin S.A., Pakhnutova N.V., Shkoda O.A., Boyangin E.N.** Experimental study of the microhardness and microstructure of a copper specimen using the Taylor impact test. *Metals*, 2022, vol. 12, no. 12, p. 2186.
4. **Min F., Gao K., Huang H., Wen S., Wu X., Nie Z., Zhou D., Gao X.** Application of the modified GTN model in predicting Taylor impact fracture of 7XXX aluminum alloy. *Computers and Structures*, 2024, vol. 301, p. 107457.
5. **Rodionov E.S., Pogorelko V.V., Lupanov V.G., Fazlitdinova A.G., Mayer P.N., Mayer A.E.** Dynamic deformation and fracture of brass: Experiments and dislocation-based model. *International Journal of Plasticity*, 2024, vol. 183, p. 104165.
6. **Wang Y., Xin L., Liu H., Su B., Jin T., Zhang S., Chen J., Li Z.** Modeling of strain hardening behaviors of 6061 aluminum alloy considering strain rate and temperature effects. *Journal of Materials Research and Technology*, 2024, vol. 30, pp. 4973–4985.
7. **Iannitti G., Bonora N., Testa G., Ruggiero A.** High-rate characterization of additively manufactured Ti-6Al-4V using Taylor cylinder impact test: Experiments. *Material Design and Processing Communications*, 2021, vol. 3, no. 5, p. e192.
8. **Kolomy S., Jopek M., Sedlak J., Benc M., Zouhar J.** Study of dynamic behaviour via Taylor anvil test and structure observation of M300 maraging steel fabricated by the selective laser melting method. *Journal of Manufacturing Processes*, 2024, vol. 125, pp. 283–294.
9. **Ricci S., Iannitti G., Testa G., Sgambetterra M., Zucca G., Ruggiero A., Gentile D., Bonora N.** High-rate characterization of L-PBF AlSi10Mg under impact conditions. *Journal of Dynamic Behavior of Materials*, 2024, vol. 11, pp. 106–118.
10. **Wang Z., Zhang T., Tang E., Xiong R., Jiao Z., Qiao J.** Formation and deformation mechanisms in gradient nanostructured NiCoCrFe high entropy alloys upon supersonic impacts. *Applied Physics Letters*, 2021, vol. 119, iss. 20, p. 201901.
11. **Sun Z., Shi C., Xiao X., Luo X., Xia Z., Yin Q.** Investigation of mechanical behavior, constitutive modeling, and fracture criteria for as-cast $Al_{0.3}$CoCrFeNi high entropy alloy. *Intermetallics*, 2023, vol. 162, p. 108029.
12. **Xu J., Liu Q., Xu Y.F., Guo S.H., Li C., Zhang N.B., Cai Y., Liu X.Y., Lu L., Luo S.N.** Taylor impact of high-entropy alloy $Al_{0.1}$CoCrFeNi: Dynamic severe plastic deformation and bulk gradient structure. *Journal of Alloys and Compounds*, 2023, vol. 936, p. 168261.
13. **Rodionov E.S., Mayer A.E.** Estimation of dynamic yield stress by Taylor test with reduced cylindrical head part of samples. *Chelyabinsk Physical and Mathematical Journal*, 2023, vol. 8, iss. 3, pp. 399–409.
14. **Piao M.J., Huh H., Lee I., Park L.** Characterization of hardening behaviors of 4130 Steel, OFHC Copper, Ti6Al4V alloy considering ultra-high strain rates and high temperatures. *International Journal of Mechanical Sciences*, 2017, vol. 131–132, pp. 1117–1129.

15. **Zelepugin S.A., Cherepanov R.O., Pakhnutova N.V.** Optimization of Johnson–Cook constitutive model parameters using the Nesterov gradient-descent method. *Materials*, 2023, vol. 16, no. 15, p. 5452.
16. **Sjue S., Ahrens J., Biswas A., Francom D., Lawrence E., Luscher D., Walters D.** Fast strength model characterization using Bayesian statistics. *AIP Conference Proceedings*, 2020, vol. 2272, p. 070043.
17. **Rivera D., Bernstein J., Schmidt K., Muyskens A., Nelms M., Barton N., Kupresanin A., Florando J.** Bayesian calibration of strength model parameters from Taylor impact data. *Computational Materials Science*, 2022, vol. 210, p. 110999.
18. **Rodionov E.S., Pogorelko V.V., Lupanov V.G., Mayer P.N., Mayer A.E.** Modified Taylor impact tests with profiled copper cylinders: Experiment and optimization of dislocation plasticity model. *Materials*, 2023, vol. 16, no. 16, p. 5602.
19. **Veysset D., Lee J.-H., Hassani M., Kooi S.E., Thomas E.L., Nelson K.A.** High-velocity micro-projectile impact testing. *Applied Physics Reviews*, 2021, vol. 8, p. 011319.
20. **Hassani M., Veysset D., Sun Y., Nelson K.A., Schuh C.A.** Microparticle impact-bonding modes for mismatched metals: From co-deformation to splatting and penetration. *Acta Materialia*, 2020, vol. 199, pp. 480–494.
21. **He L., Veysset D., Nault I.M., Champagne V.K., Hassani M.** Impact and bonding behavior of core-shell powder particles. *Surface and Coatings Technology*, 2022, vol. 441, p. 128591.
22. **Lucas T.J., Saunders A.M., Schuh C.A.** Microstructure effects on high velocity microparticle impacts of copper. *Acta Materialia*, 2024, vol. 280, p. 120329.
23. **Hassani M., Veysset D., Sun Y., Nelson K.A., Schuh C.A.** Material hardness at strain rates beyond $10^6\,\mathrm{s}^{-1}$ via high velocity microparticle impact indentation. *Scripta Materialia*, 2020, vol. 177, pp. 198–202.
24. **Nguyen T., Fensin S.J., Luscher D.J.** Dynamic crystal plasticity modeling of single crystal tantalum and validation using Taylor cylinder impact tests. *International Journal of Plasticity*, 2021, vol. 139, p. 102940.
25. **Feng Z., Zecevic M., Knezevic M., Lebensohn R.A.** Predicting extreme anisotropy and shape variations in impact testing of tantalum single crystals. *International Journal of Solids and Structures*, 2022, vol. 241, p. 111466.
26. **Plimpton S.** Fast parallel algorithms for short–range molecular dynamics. *Journal of Computational Physics*, 1995, vol. 117, no. 1, p. 1–19.
27. **Thompson A.P., Aktulga H.M., Berger R., Bolintineanu D.S., Brown W.M., Crozier P.S., Veld P.J., Kohlmeyer A., Moore S.G., Nguyen T.D., Shan R., Stevens M.J., Tranchida J., Trott C., Plimpton S.J.** LAMMPS — a flexible simulation tool for particle-based materials modeling at the atomic, meso, and continuum scales. *Computer Physics Communications*, 2022, vol. 271, p. 108171.
28. **Mishin Y., Mehl M.J., Papaconstantopoulos D.A., Voter A.F., Kress J.D.** Structural stability and lattice defects in copper: Ab initio, tight-binding, and embedded-atom calculations. *Physical Review B*, 2001, vol. 63, iss. 22, p. 224106.
29. **Daw M.S., Baskes M.I.** Embedded-atom method: Derivation and application to impurities, surfaces, and other defects in metals. *Physical Review B*, 1984, vol. 29, p. 6443.
30. **Stukowski A.** Visualization and analysis of atomistic simulation data with OVITO — the Open Visualization Tool. *Modelling and Simulation in Materials Science and Engineering*, 2010, vol. 18, no. 1, p. 015012.
31. **Stukowski A., Bulatov V.V., Arsenlis A.** Automated identification and indexing of dislocations in crystal interfaces. *Modelling and Simulation in Materials Science and Engineering*, 2012, vol. 20, no. 8, p. 085007.
32. **Larsen P.M., Schmidt S., Schiøtz J.** Robust structural identification via polyhedral template matching. *Modelling and Simulation in Materials Science and Engineering*, 2016, vol. 24, no. 5, p. 055007.

33. **Mayer A.E., Krasnikov V.S., Pogorelko V.V.** Homogeneous nucleation of dislocations in copper: Theory and approximate description based on molecular dynamics and artificial neural networks. *Computational Materials Science*, 2022, vol. 206, p. 111266.
34. **Mayer A.E., Lekanov M.V., Grachyova N.A., Fomin E.V.** Machine-learning-based model of elastic-plastic deformation of copper for application to shock wave problem. *Metals*, 2022, vol. 12, iss. 3, p. 402.
35. **Grachyova N.A., Fomin E.V., Mayer A.E.** Theoretical model of structural phase transitions in Al-Cu solid solutions under dynamic loading using machine learning. *Dynamics*, 2024, vol. 4, iss. 3, pp. 526–553.

Article received 07.10.2024.
Corrections received 29.11.2024.

Челябинский физико-математический журнал. 2025. Т. 10, вып. 4. С. 801–812.

УДК 539.3 DOI: 10.47475/2500-0101-2025-10-4-801-812

МОЛЕКУЛЯРНО-ДИНАМИЧЕСКОЕ МОДЕЛИРОВАНИЕ УДАРНЫХ ИСПЫТАНИЙ ТЕЙЛОРА С КЛАССИЧЕСКИМИ И ПРОФИЛИРОВАННЫМИ МЕДНЫМИ ЦИЛИНДРАМИ

А. Е. Майер[a], Е. С. Родионов[b], В. В. Погорелко[c], П. Н. Майер[d]

Челябинский государственный университет, Челябинск, Россия
[a]mayer@csu.ru, [b]rodionoves.pgd@gmail.com, [c]vik_ko83@mail.ru, [d]polina.nik@mail.ru

Тесты Тейлора, предполагающие высокоскоростной удар образцов о жёсткую наковальню, широко используются для изучения динамического отклика различных металлических материалов. Чтобы расширить наши предыдущие экспериментальные исследования и выявить особенности тестов Тейлора в наномасштабе, здесь мы проводим молекулярно-динамическое моделирование для монокристаллической и поликристаллической меди, рассматривая как классические цилиндрические образцы, так и профилированные образцы с уменьшенной головной частью. Геометрическая форма образцов аналогична той, которая использовалась в экспериментах, но общая длина составляет 80 или 200 нм в отличие от образцов длиной 40 мм в экспериментах. Несмотря на разницу в пять порядков по длине, рассчитанные методом МД кривые относительной длины после удара в зависимости от скорости удара аналогичны экспериментально измеренным для миллиметровых образцов, но, как и ожидалось, показывают гораздо более высокую прочность наноразмерных образцов. Как монокристаллические, так и поликристаллические образцы подвержены потере исходной цилиндрической симметрии в процессе удара. В случае монокристалла это происходит из-за активации определённых систем скольжения. В случае поликристаллов это связано с анизотропией отдельных зёрен и отчётливо проявляется, когда профилированная часть образца содержит всего несколько зёрен по толщине. Эта потеря симметрии коррелирует с искажением формы профилированных образцов в наших экспериментах с отожжённой крупнозернистой медью, в которой наиболее крупные зёрна достигают миллиметровых размеров. Таким образом, наблюдаемое в эксперименте искажение симметрии имеет фундаментальную причину локализации пластического течения.

Исследование выполнено при финансовой поддержке Российского научного фонда, проект № 20-11-20153-P, https://rscf.ru/en/project/23-11-45024/.

Ключевые слова: *испытание на удар по Тейлору, наноразмерный образец, молекулярная динамика, динамическая пластическая деформация, медь, монокристалл, поликристалл, потеря симметрии, локализация пластической деформации.*

Поступила в редакцию 07.10.2024.
После переработки 29.11.2024.

Сведения об авторах

Майер Александр Евгеньевич, доктор физико-математических наук, доцент, заведующий кафедрой общей и теоретической физики, Челябинский государственный университет, Челябинск, Россия; mayer@csu.ru.

Родионов Егор Сергеевич, кандидат физико-математических наук, заведующий учебной лабораторией общей и прикладной физики кафедры общей и теоретической физики, Челябинский государственный университет, Челябинск, Россия; rodionoves.pgd@gmail.com.

Погорелко Виктор Владимирович, кандидат физико-математических наук, доцент кафедры общей и теоретической физики, Челябинский государственный университет, Челябинск, Россия; vik_ko83@mail.ru.

Майер Полина Николаевна, кандидат физико-математических наук, доцент кафедры общей и теоретической физики, Челябинский государственный университет, Челябинск, Россия; polina.nik@mail.ru.